Chapter 2

Data-driven methods for vibration-based monitoring based on singular spectrum analysis

Irina Trendafilova*, David Garcia and Hussein Al-Bugharbee

Department of Mechanical and Aerospace Engineering,
University of Strathclyde, UK
**irina.trendafilova@strath.ac.uk*

This chapter studies the application of data-driven methods and specifically principal component analysis (PCA) and singular spectrum analysis (SSA) for purposes of damage assessment in structures and machinery. In this study, data analysis methods PCA and SSA are applied to the measured vibration signals in order to extract information about the state of the structure/machinery and the presence of a fault in it. Two applications are offered, one for damage assessment on a wind turbine blade and another one for fault diagnosis in rolling element bearings. The results demonstrate strong capabilities of the investigated methodology for both structural damage detection and rolling element fault diagnosis. Eventually, a discussion about the capabilities of the studied methodology and the way forward regarding extending its capabilities and applications is offered.

Nomenclature

$\mathbf{A}_k$	kth principal component
$\mathbf{A}$	principal component matrix
$\mathbf{C}_\mathrm{X}$, $\mathbf{C}_\mathrm{Y}$	covariance of $\tilde{\mathbf{X}}$ and $\tilde{\mathbf{Y}}$
$D_\mathbf{i}$	damage index of an ith observation feature vector
$\mathbf{E}^k, \mathbf{U}_k$	kth eigenvectors
$\mathbf{E}_\mathrm{Y}, \mathbf{U}$	eigenvectors matrix
$\mathbf{E}_\mathrm{Y}^\mathrm{t}$	transpose matrix of $\mathbf{E}_\mathrm{Y}$
ϑ	threshold value
$\mathbf{H1}, \mathbf{H2}$	hypotheses of decision making
i	variable of an observation feature vector index

j	variable of a feature vector index
k	eigenvalue and eigenvector index
K	length of embedding matrix $\tilde{\mathbf{X}}$
$\lambda_k, \mathbf{\Lambda}^k$	kth eigenvalue
$\mathbf{\Lambda}_Y$	eigenvalue matrix
M	number of signal vector realizations
m	signal realizations index
μ_B	mean vector of each FV in $\mathbf{T}_B$
N	length of the signal $\mathbf{x}$
$\bar{\text{N}}$	length of the signal $\mathbf{y}$
n	variable index of length
l	sliding window size index
L	sliding window size
L_n	normalization factor
p	reduced dimension of the feature space
$\mathbf{\Sigma}^{-1}$	inverse of covariance matrix of $\mathbf{T}_B$
$\mathbf{R}$	full reconstructive components matrix
s	variable of a baseline feature vector index
T_j	variable of a feature vector
$\mathbf{T}$	feature vector
$\mathbf{T}_B$	baseline feature vector matrix
$\mathbf{T}^i$	observation feature vector
$\mathbf{x}$	signal vector in time domain
$\mathbf{x}_m$	signal vector realization m in time domain
$\tilde{\mathbf{X}}$	full embedding matrix of $\mathbf{x}$
$\tilde{\mathbf{X}}^t$	transpose of full embedding matrix
$\mathbf{y}_m$	signal vector realization m in frequency domain
$\tilde{\mathbf{Y}}_m$	embedding matrix of $\mathbf{y}_m$
$\tilde{\mathbf{Y}}$	full embedding matrix
$\tilde{\mathbf{Y}}^t$	transpose of full embedding matrix $\tilde{\mathbf{Y}}$

1. Introduction

In this section, the main idea of vibration-based monitoring as applied to structures and machinery will be discussed. Then, data-driven methods will be introduced and their place among the vibration-monitoring (VM) methods will be discussed. Later, the focus will be placed on principal component analysis (PCA) and singular spectrum analysis (SSA) and the way these can be applied to structural and machinery damage and fault assessment.

Structural health monitoring (SHM) plays an important role in the inspection of the structural integrity of most advanced materials. Most structures are subjected to vibrations, and therefore vibration-based SHM (VSHM) methods present an attractive possibility for monitoring.

Analogically, fault inspection and monitoring is an integral part for most complex machinery. Most machines vibrate during their operation and for them VM is one of the most widely used monitoring methods.

The background of VSHM and VM is in the fact that any change introduced within the structure/machine result in changes in its vibration response. Accordingly, a fault or damage within the structure/machine will incur changes in the vibration response no matter whether one is looking at the free or a forced vibration response. The important characteristics of VSHM and VM methods are that they are global and as such can be used to inspect parts which are difficult or impossible to access and also can be applied when the location of the damage fault is not known in advance.

In general there are two types of vibration-based monitoring methods depending on their nature: model-based ones and non-model based or data-driven methods.[1] The first type of methods rely on a model for the structure/machinery inspected and generally compare the modeled and the recorded vibration responses and, on the basis of this, extract information about the presence of a fault/damage, its location and/or its extent. Currently and historically, most structural and machine dynamic models assume some level of linearity, some models are even totally linear in the sense that they assume linear dynamic as well as linear material/structural behaviors. Unfortunately, most machines and structures demonstrate quite well-expressed nonlinear behavior as result of nonlinearities due to: material (e.g. in the case of composite materials), boundary conditions or nonlinearities that come from the structure and the connections. On some occasions even though the structure or the machine demonstrates nonlinear dynamic behavior, the linear model can still present a good approximation. But, in a number of cases, especially for cases of strong/distributed nonlinearities (as is the case for composite materials and/or complex machinery), the nonlinearities cannot be neglected, and hence the linear approximation cannot be considered as a good alternative. Using nonlinear modeling and applying it further for damage assessment is a rather complicated task and it has its challenges and limitations. On a number of occasions even though the model attempts to take into account the nonlinearities of the structure, the modelled response might still be different from the measured one. Then,

an updating process might regard these differences as damage/fault-caused ones. On the contrary, *data-driven* methods do not assume any model or linearity. They just regard the measured signals as data and use certain data transformations in order to extract information from this data. The data-driven methods have become quite popular recently for the purposes of structural and machine VM.[1,2] They have demonstrated their capabilities for addressing the problems for damage detection and identification.[3] Most data-driven methods eventually classify the measured data to two or more categories (e.g. healthy and damaged).

Most data-driven structural and machinery diagnosis methods include three main stages: Stage 1, *Data acquisition*, Stage 2, *Signal analysis*, and Stage 3, *Diagnosis*. *Data acquisition* is the process of collecting useful information (i.e. signal) about the system. In this step, the number, type, locations, and sensitivity of the sensors to collect the signal are determined. The *signal analysis* step includes subjecting the signal to certain pretreatment and extracting some compact information, which might be in the form of "features" which are further used for monitoring the health status of the structure/machinery or for distinguishing among different health conditions. *Diagnosis* is the step in which the structure/machinery is assigned a category corresponding to one of the possible health conditions (e.g. healthy and damaged/faulty).

There are two main types of data-driven methods according to the type of classification procedure that they use for the purposes of damage assessment. The first type of methods are those that only use the data from the healthy state for the purposes of damage diagnosis, and these are the so-called un-supervised methods. The second type of methods utilize data from the healthy and the damaged states and make the decision on the basis of these two or more data categories; these are referred to as supervised methods. The first type of methods generally use the outlier principle in order to detect damage. Such methods are generally only capable of damage detection (Level one) and they need additional procedures in order to distinguish between different data categories stemming from different damage/fault types or sizes. The supervised type of methods are generally capable to do the higher stages of a monitoring method in terms of diagnosis.

Depending on the level of diagnosis, the classification might distinguish between two groups only (healthy and faulty) or can be extended to classify the structural/machinery condition to more than two categories (like e.g. corresponding to the fault size or the fault type). Many studies use

classification/categorization process to perform the diagnosis, and many others apply pattern recognition for the purposes of detection and diagnosis.[3] The simplest way of distinguishing between two or sometimes more categories is to use a threshold-based method. Then, a certain variable/feature is measured and if it is below the threshold, the structure/machinery is considered healthy. Once the feature exceeds the threshold, the structure/machine passes into faulty/damaged state. This can be extended to more than two categories if multiple thresholds are used that might correspond to different fault/damage extensions.[4] Different pattern recognition techniques can be used for the purpose of recognition between two or more structural/machinery states. A lot of authors suggest neural networks-based classifiers for this purpose.[5] For the signal analysis stage, a number of transformations can be used, which range from the simplest ones that estimate some statistical moments to much more complicated ones that use, e.g. regressive and autoregressive modeling.[6] These include, e.g. extracting some statistical features and assessing their values at different structural/machinery conditions. Kurtosis and crest factor are two of the most commonly used features in machinery fault diagnosis problems. Both these factors characterize the "peakiness" of a signal. Some studies basically use the frequency domain vibration signal where the repetitive signal components will correspond to peaks at the frequency of repetition. Furthermore, the signal can be divided into different frequency bands, and/or some frequency bands may be filtered depending on the frequency ranges of interest.[7]

The data-driven methods usually use time series analysis methods in order to transform the measured data and extract information for the presence of a fault/damage and for its type and size.[8,9] A time series can be defined as a sequence of measurements of a time-dependent variable, e.g. acceleration or velocity, collected over a number of discrete time points. The concept of time series analysis is very popular in climate and financial research fields[10] and a large number of techniques have been developed for purposes of analysis or predicting of the future values of time series. These techniques take into account some aspects of the internal structure in the data. Some of these techniques offer representing a time series by parametric models such as autoregressive (AR) modeling.[11] Others, such as the SSA[12] are used to decompose time series into a number of independent components that can have some meaningful interpretation such as trend and periodic components.

This study describes two methods that were developed for two different purposes, for structural health monitoring and for machinery fault

diagnosis. In the latter case, the machinery faults to be identified are rolling element bearing faults. Both methods are data driven and both use SSA in different forms, as part of the methodologies, for structural and machinery fault/damage diagnosis.

2. PCA and SSA and Their Application for the Purposes of Structural and Machinery Monitoring

PCA is a data analysis technique that has been quite extensively used for the analysis of climatological, medical, and financial data. It found popularity recently in engineering and especially for the purposes of structural and machinery monitoring. The main idea of PCA is to reduce the data dimensionality while at the same time retaining most of its variance.[13] It has some attractive properties which are beneficial for applications within the field of vibration-based monitoring. PCA decomposes the original data into a number of independent components, the first several of which contain most of the data variance. For the case of data from multiple categories, the new variables, the principal components (PCs), tend to be grouped according to these categories, as PCA tends to reduce the distance between data from the same category while at the same time increasing the distance between data from different categories. These properties make PCA useful for the analysis of data coming from e.g. different damage states. There are a number of papers that suggest the application of PCA for structural and machinery monitoring purposes.[14–17] Several investigations suggest the selection of certain features from the time or frequency domain of the vibration response signals, which can be considered as independent, and subjecting them to PCA.[18] On most occasions, these are certain frequency components which, e.g. correspond to peaks in the spectrum or time components that are far enough from each other to be considered independent. Some studies use the natural frequencies as initial data and decompose them into PCs.[19] In some papers, PCA is applied twice — once on the initial data and a second time on the decomposed data.[20] The authors suggest that this is useful for excluding the variability due to the environment and the operational conditions. As the first several PCs retain a high proportion of the variance, some authors argue that they also retain most of the useful information about the structure, embedded in the data analyzed, and accordingly they suggest the use of the few first principle components for the purposes of vibration analysis and vibration-based damage assessment. Other investigations suggest that the higher PCs containing the smallest amount of variance will contain

information about the presence of damage, and accordingly suggest to use these in order to form damage features.[21] These studies propose that the first PCs are mostly responsible for the noise within the data rather than its internal structure and thus conclude that the last PCs are likely to contain most of the useful information about the structural/machinery dynamics.

SSA is a variation of PCA which has been developed especially for time series analysis. PCA regards the initial data as statistically independent. For the case of time series, two or more consecutive time series, components are not independent on most occasions as there is common information contained in these components, i.e. they contain "mutual information". SSA is designed to deal with non-independent data. SSA can be applied in the time and the frequency domain.[13] The aim of SSA is to decompose the original signal using a small number of independent and more interpretable components which can be used for trend identification, detection of oscillatory components, periodicity extraction, signal smoothing, noise reduction, feature extraction, and detection of structural changes in the time series. SSA has been applied for diverse applications ranging from weather forecasting[22] and financial mathematics[12] to historical[23] and economical time series where the signals are highly non-stationary with no signs of periodicities.[24]

SSA considers all rotational patterns contained in the vibration response rather than those corresponding to a particular frequency. For this reason, when SSA is applied to a time domain vibration signal, the signal is decomposed into harmonic and non-harmonic oscillatory components. Hence, SSA can be regarded as a kind of nonlinear spectral analysis.[25] This is why it can be argued that close modes, which are a feature of many nonlinear dynamic systems, will not be lost when SSA is used for decomposition purposes. There are a small number of publications related to the application of SSA for structural vibration analysis and for vibration-based SHM. In Ref. 26, SSA is applied for structural monitoring and damage diagnosis in bridges by using an eigenvalue ratio difference between the first two eigenvalues. Thus, when the difference between the first two eigenvalues increases, it can be considered as an indication for the occurrence of an irregularity. In the same study, the residual errors were measured by comparing the reconstructed vibration responses based on the SSA decomposition with the measured ones. In Ref. 27, the performance of an SSA-based methodology was compared to another method covariance-driven stochastic subspace identification (SSI-COV), and the authors claim the superiority of the SSA-based method in terms of speed and precision.

SSA has been applied in a couple of studies featuring machinery vibration-based fault diagnosis.[16,28–30] Bubathai[30] published the first study which uses SSA for classifying rolling element bearing signals as healthy and faulty (with a fault on inner raceway) for detection purposes only. In this study, the vibration acceleration signals from both categories were subjected to SSA and the original signals are decomposed into two PCs: trend and residuals. Then, only the trend component was considered for further analysis. A number of statistical features such as peak value and the standard deviation are obtained from the trend. These features are further used to form the feature vectors (FVs) which are eventually used as input for a neural network classifier. SSA was used as a multi-decomposition analysis technique.[16] In this study the number of singular values, which preserves a specific predetermined variance percentage, is used as an indicator for fault presence. Two different feature sets were obtained from the application of SSA[17] and used as FVs. The first FV was made of the singular values and the second one- from the energy of the first time domain PCs. The bearing condition classification was performed by using those FVs as input to a back propagation neural network classifier.

This chapter considers the application of SSA for two different purposes, namely, for structural health monitoring purposes as applied for delamination detection in wind turbine blades and for the purposes of machinery fault diagnosis as applied for rolling element fault identification.

The first application for structural health monitoring purposes decomposes the frequency domain signal rather than the measured time series. The argument for this is that a frequency domain representation presents the oscillatory patterns contained in the vibration response in more interpretable and ordered manner. It uses all the steps of SSA — decomposes and after that reconstructs the initial signal. The reconstructed signal demonstrates very good agreement with the original one, from which one can conclude that the used decomposition has preserved most of the important signal characteristics and the information contained within the signal by using a reduced number of reconstructive components. When the methodology is performed in the frequency domain, it can be observed that the first reconstructive component contains the general trend of the spectral line and the rest of reconstructive components contain the fluctuations along the spectral line. Therefore, only reduced number of reconstructive components is needed to describe the general behavior of the spectral line.[31−32] Most authors who suggest application of SSA apply this to the original time domain signal.[33]

The second application is for rolling element fault diagnosis. In this application, the time domain signal representation is used. This application

suggests a classification process in order to first detect the presence of a fault and then identify the fault type and eventually estimate the fault size. Very little rolling element fault assessment studies offer a complete identification in terms of detection, type assessment, and extent estimation. This is one of the main contributions of this second application of SSA. The whole process suggested is very easy and can be made automatic so that it can be used for practical fault identification. This identification process uses only the first stage of SSA — the signal decomposition into PCs in order to extract fault features and assess the fault. This is the second important advantage of the suggested methodology for machinery diagnosis. It uses the signals corresponding to the baseline condition and decomposes them into PCs. A number of the first PCs are chosen, according to the percentage of variance they contain, and a baseline space is created using these first several PCs. Subsequently any of the signal that have to be identified are only projected on the baseline space in order to be compared to the healthy state. Most methods that use SSA for structural and machinery monitoring purposes use all the three stages of the process — the embedding, the decomposition, and the reconstruction stage. Thus, it should be noted that the method presented here is actually much simpler as it contains less computation, which makes it quite easy for application purposes. The SSA decomposition divides the data into categories which are well distinguishable and can be assigned to the different fault types and fault sizes. It should also be mentioned that the methods developed and described in this study give a very good and correct classification rate. The rolling element fault diagnosis method was compared in terms of performance to some other methods that were applied for the same data and it is observed that it outperforms them.

The next paragraph introduces the two methods — the one for structural health monitoring and the method for bearing fault diagnosis. The following two paragraphs are dedicated to two particular applications of the introduced methodologies. They introduce the case studies, the experiments performed, the data collected, as well as the transforms applied. They also introduce some results from both applications and offer a short analysis of these results. The last section of this chapter suggests a discussion of the developed methods and the results obtained for the two case studies.

3. Two SSA-based Damage Assessment Methodologies for Structural and Machinery Monitoring

This section introduces two damage assessment methodologies as developed for structural health monitoring and for rolling element fault diagnosis.

As mentioned before, both methods are based on SSA decomposition, but they use different modifications of SSA and are applied in different ways. The first method is applied for structural health monitoring and it uses the signal in the frequency domain. The second method is developed for rolling element bearing diagnosis and it decomposes the time domain signal. The rationale behind this is that for the first case, most of the information regarding the vibration modes of the structure needed to be retained, while in the second case it is assumed that most of the information about the system can be recovered using the lagged time signals. In this paragraph, the basic steps of SSA are first introduced and then the two methods for damage assessment as applied for different purposes are presented.

3.1. *SSA basic steps*

SSA, as a decomposition method, has several major stages, namely, data collection, embedding, decomposition, and reconstruction.[34] The method for structural damage assessment considered here uses all these three steps. The method for bearing fault diagnosis discussed below does not follow the reconstruction stage.[35] The latter creates a reference space related to the healthy state based on the decomposed components only.

3.1.1. *Data collection*

In general, SSA as well as PCA are data analysis methods and they assume multiple realizations of the signal in their analysis process, which might be taken in different locations or just as a result of a number of measurements. In this study, the data collection is done in different ways for the SHM process, and for machinery monitoring procedure. In the SHM process, the acceleration signal is measured in a number of different positions. In the second application, a long enough signal is measured and it is later on divided into segments which are treated as different realizations/measurements. For the purposes of data collection, the measured signals are initially arranged into a matrix as columns.

3.1.2. *Embedding*

The embedding stage in SSA is used to embed a lagged version of the measured signal into a matrix, thus expanding the information contained in the signal into more dimensions according to Takens embedding theorem.[36]

Embedding can be done in different ways, but in all cases a window of certain size, smaller than the original size of the signal, is used and each signal vector is embedded (expanded) into a matrix using lagged versions of the vector itself. Generally speaking, as a result of the embedding each signal/vector is transformed/unfolded into a matrix. Usually, the embedding is performed in the time domain, but it might be done in the frequency domain as well, if SSA is applied on the signal spectra rather than on the time signature. Eventually, the embedding is done for all the data vector realizations, and the corresponding matrices are put together to form the final data matrix, also called an embedding matrix, which is subjected to the second step, i.e. the PCs decomposition. In this study, two different embedding procedures are used for the development of the two methods, as is presented in the following sections. One of the methods is applied on the frequency domain signal representation and the other one on the original time domain.

3.1.3. *Decomposition*

The decomposition into PCs is performed using the covariance matrix of the embedding matrix. The covariance matrix gives the covariance between the signal realizations. This covariance matrix is then subjected to eigen value decomposition to obtain its eigenvalues and eigenvectors. Each eigenvalue represents the partial variance of the original time series in the direction of the corresponding eigenvector. Projecting the embedding matrix onto each eigenvector provides the corresponding PCs.

3.1.4. *Reconstruction*

The idea of this stage is to reconstruct the original signal using a linear combination of the obtained PCs. The original signals can be reconstructed by a linear combination of all or just a few of the PCs. Different criteria can be used to select the number of PCs to be used in the reconstruction process. As a result, the so-called reconstructed components (RCs) are obtained. Using a number of or all the reconstructed components, the original signal can be reconstructed with certain accuracy. A good agreement between the original and the reconstructed signal (small difference error) means that the decomposition process was able to capture most of the information contained in the original data.

3.2. *Development of an SSA-based technique as a methodology for VSHM*

This method follows the general steps of SSA as explained above, which are the data collection, the embedding, the decomposition into PCs, and the reconstruction. The main stages involved in the diagnosis are: (1) creation of reference space relative to which all the new signals will be compared and (2) damage detection. The reference space is created using SSA. The recognition between healthy and faulty structures is done by comparing each set of new data to the baseline/healthy set of data which is transformed into new coordinates in order to create the baseline/reference space. A new signal is then projected onto the reference space and is classified as healthy or damaged based on a predefined threshold.

In the following sections, the main steps of the method are briefly described.

3.2.1. *Data collection*

A discrete acceleration signal is measured in N time sampling points. Each signal is standardized to have a zero mean and unit variance. As mentioned above, one is in possession of a number $m = 1, \ldots, M$ of realizations of such acceleration signals, each of which can be represented by a signal vector as shown in Equation (1):

$$\mathbf{x}_m = (x_{1,m}, x_{2,m}, \ldots, x_{N,m}) \tag{1}$$

Each signal vector $\mathbf{x}_m$ is then transformed to the frequency domain to obtain a new signal vector $\mathbf{y}_m$ with a length $\bar{N} = N/2$. All the obtained frequency domain signal vectors are stored into a matrix $\mathbf{Y}$ as shown in Equation (2).

$$\mathbf{Y} = (\mathbf{y}_1, \mathbf{y}_2, \ldots, \mathbf{y}_M) \tag{2}$$

3.2.2. *Creation of the reference space*

A reference space is built using the signals, measured on the healthy/pristine structure. The steps for creating the reference space are: Embedding, decomposition, and reconstruction. Each of these steps is briefly described below.

1 3.2.2.1. Embedding

This step creates an embedded matrix of the signal vector $\mathbf{y}_m$. Each signal vector $\mathbf{y}_m$ is embedded into a matrix $\tilde{\mathbf{Y}}_m$ by using L lagged copies of the signal/vector itself as shown in Equation (3), where L is the sliding window size.

$$\tilde{\mathbf{Y}}_m = \begin{pmatrix} y_{1,m} & y_{2,m} & y_{3,m} & \cdots & y_{L,m} \\ y_{2,m} & y_{3,m} & y_{4,m} & \cdots & y_{(L+1),m} \\ y_{3,m} & y_{4,m} & y_{5,m} & \cdots & \vdots \\ y_{4,m} & y_{5,m} & \vdots & \cdots & \vdots \\ y_{5,m} & \vdots & \vdots & \cdots & y_{\bar{N},m} \\ \vdots & \vdots & y_{(\bar{N}-1),m} & \cdots & 0 \\ \vdots & y_{(\bar{N}-1),m} & y_{\bar{N},m} & \cdots & 0 \\ y_{(\bar{N}-1),m} & y_{\bar{N},m} & 0 & \cdots & 0 \\ y_{\bar{N},m} & 0 & 0 & \cdots & 0 \end{pmatrix} \tag{3}$$

The embedding process is applied to each signal/vector and then all $\tilde{\mathbf{Y}}_m$ matrices are used to create the data-embedded matrix $\tilde{\mathbf{Y}}$ given by Equation (4). The dimension of the matrix $\tilde{\mathbf{Y}}$ is $[\bar{N} \times (ML)]$. The sliding window size L is usually selected so that $M < L$ and $L \leq \bar{N}/2$.

$$\tilde{\mathbf{Y}} = (\tilde{\mathbf{Y}}_1, \tilde{\mathbf{Y}}_2, \ldots, \tilde{\mathbf{Y}}_M) \tag{4}$$

2 3.2.2.2. Decomposition into PCs

The embedding matrix $\tilde{\mathbf{Y}}$ obtained above (see Equation (4)) is decomposed into PCs. First, the covariance matrix $\mathbf{C_Y}$ of the matrix $\tilde{Y}$ is calculated according to Equation (5).

$$\mathbf{C}_Y = \frac{\tilde{\mathbf{Y}}^{\mathrm{t}}\tilde{\mathbf{Y}}}{N} \tag{5}$$

where $\tilde{\mathbf{Y}}^{\mathrm{t}}$ is the transpose matrix of $\tilde{\mathbf{Y}}$. The covariance matrix $\mathbf{C}_Y$ has a dimension $[(ML) \times (ML)]$ and gives the covariance between signal realizations. The matrix $\mathbf{C}_Y$ is subsequently subjected to eigenvalue decomposition as shown in Equation (6):

$$\mathbf{E}_Y^t \mathbf{C}_Y \mathbf{E}_Y = \mathbf{\Lambda}_Y \tag{6}$$

The matrix $\mathbf{\Lambda}_{\mathrm{Y}}$ is a diagonal matrix with eigenvalues λ_{k} on its diagonal in decreasing order and $\mathbf{E}_{\mathrm{Y}}$ contains all eigenvectors $\mathbf{E}^k$ in columns in the same order as the corresponding eigenvalues. Each eigenvector $\mathbf{E}^k$ is composed of M consecutive L-long segments, depending on the number of realizations and the sliding window size, respectively, with its elements denoted by $E^k_{m,l}$. Each PC $\mathbf{A}_k$ associated with each eigenvector $\mathbf{E}^k$ is a single-channel vector calculated by projecting the matrix $\tilde{\mathbf{Y}}$ onto $\mathbf{E}_{\mathrm{Y}}$ as shown in Equation (7) where $n = 1, \ldots, \bar{N}$ (see Ref. 22).

$$A^k_n = \sum_{l=1}^{L} \sum_{m=1}^{M} Y_{m,n+l} E^k_{m,l} \tag{7}$$

Accordingly, it can be seen from Equation (7) that each PC contains characteristics from all the M signal vector realizations.

3.2.2.3. Reconstruction

For a given set of indices K, the RCs are calculated by convolving the PCs with the eigenvectors $\mathbf{E}_{\mathrm{Y}}$, so that the kth RC at n-value for an m-realization is given by Equation (8) where $n = 1, \ldots, \bar{N}$ (see Ref. 22).

$$R^k_{m,n} = \frac{1}{L_n} \sum_{l=1}^{L} A^k_{n-l} E^k_{m,l} \tag{8}$$

Each $\mathrm{R}^k_{m,n}$ value is normalized by a normalization factor L_n which is shown in Equation (9):

$$L_n = \begin{cases} n & 1 \leq n \leq L-1 \\ L & L \leq n \leq N \end{cases} \tag{9}$$

The matrix $\mathbf{R}$ includes all reconstructed components for all the original signal vectors in columns.

3.2.3. *Feature extraction*

A FV is obtained for each newly observed signal which will be subjected to the damage assessment process, by comparing its similarity to the reference space. The FV is calculated by multiplying/projecting the observed signal vector $\mathbf{y}$ to the reference space matrix $\mathbf{R}$ as shown in Equation (10) below where $j = 1, \ldots, L$.

$$T_j = \sum_{n=1}^{\bar{N}} y_n R_{n,j} \tag{10}$$

Then, the features T_j are arranged into a vector $\mathbf{T}$ with dimension L. The FV $\mathbf{T}$ characterizes the similarity of the observed signal $\mathbf{y}$ to the reconstructed reference space.

3.2.4. *Damage assessment*

The damage assessment in this study is done on the basis of a predetermined threshold.

First a baseline feature matrix $\mathbf{T}_{\mathrm{B}}$, with a dimension $p \times s$ where p is the dimension of each FV $\{\mathbf{T}{:}p \leq L\}$ and s is the number of signal vectors used to define the baseline matrix, is created whose elements are obtained following Equation (11).

$$\boldsymbol{T}_B = \begin{pmatrix} T_{1,1} & T_{2,1} & \cdots & T_{p,1} \\ T_{1,2} & T_{2,2} & \cdots & T_{p,2} \\ \vdots & \vdots & \cdots & \vdots \\ T_{1,s} & T_{2,s} & \cdots & T_{p,s} \end{pmatrix} \tag{11}$$

The next step is to measure the similarity of an observed FV $\mathbf{T}^i = (T_{1,i}, T_{1,i}, \ldots, T_{p,i})$ to the baseline feature matrix $\mathbf{T}_B$ where i is the number of observation signal vectors considered. This is done on the basis of the Mahalanobis distance between the FV and the baseline matrix which is defined in Equation (12).

$$D_i = \sqrt{\left(\boldsymbol{T}^i - \boldsymbol{\mu}_B\right)^t \sum^{-1} \left(\boldsymbol{T}^i - \boldsymbol{\mu}_B\right)} \tag{12}$$

where $\boldsymbol{\mu}_B$ is the mean row of the baseline feature matrix $\mathbf{T}_B$ and $\boldsymbol{\Sigma}$ is its covariance matrix.

For the purposes of damage assessment, a threshold ϑ is defined and the above distance is compared to the threshold. If the distance to the baseline matrix is $D_i < \vartheta$, then the observed signal vectors are assigned to the baseline (healthy) category. If $D_i > \vartheta$, then the newly observed vector is considered to be outside the baseline category, i.e. it belongs to the damaged category.

3.3. *An SSA-based technique for rolling element fault diagnosis*

The method presented here was developed for the purposes of rolling element fault detection and diagnosis. This is a relatively simple methodology

which also uses SSA for the purposes of decomposition of the measured vibration signals. In this case, the acceleration signals are measured on bearing housing and the time domain signals are used.

The methodology decomposes the signal vectors corresponding to the healthy bearing state using an SSA-based technique in order to build a baseline space. In this case, the data collection and the decomposition stages are only used and are only applied to a set of signals which are collected in the healthy/baseline condition of the bearings.

The eigenvectors obtained applying the SSA decomposition are used to calculate the PCs corresponding to the baseline/healthy condition of the bearings. A baseline space corresponding to healthy bearings' state is created. In this way, SSA is only used to transform the baseline signals. The new signals which have to be classified as healthy or damaged are not transformed, they are just projected onto the baseline space, and these projections are used for the purposes of fault detection.

The methodology consists of three basic phases, namely fault detection, fault type identification and fault severity estimation. In the fault detection phase, the signals are classified into two categories: baseline/healthy and non-baseline/faulty. In the second phase, the fault type is identified by assigning the signals to one of fault type categories: inner race fault (IRF) and outer race fault (ORF). In the consequent fault severity estimation phase, the severity of the fault is estimated by assigning the signals to categories corresponding to different fault severity levels.

The method can be divided into two main stages: building a baseline space and fault diagnosis. An SSA-based procedure is used to build the baseline/healthy space using the signals measured on the healthy bearings, and this is described in the next paragraph.

3.3.1. *Building the baseline space*

The baseline space construction uses an SSA procedure which is applied on the vibration signals $\mathbf{x}$ measured on the healthy bearings. It contains similar phases as the procedure described in the previous section, but only the data collection and the decomposition stages are used.

3.3.1.1. Data collection and embedding

The discrete acceleration signals are measured and collected in their time domain form so that each signal is represented as a vector $\mathbf{x}$ as introduced in Equation (1) (see Section 3.2.1).

Then, the embedding stage is performed to obtain the data embedding matrix $\tilde{\mathbf{X}}$ with dimension $(L \times K)$ where L is the sliding window size and $K = N - L + 1$, as shown in Equation (13) below.

$$\tilde{\mathbf{X}} = \begin{pmatrix} x_1 & x_2 & x_3 & \cdots & x_{\mathrm{K}} \\ x_2 & x_3 & x_4 & \cdots & x_{K+1} \\ x_3 & x_4 & x_5 & \cdots & x_{K+2} \\ \vdots & \vdots & \vdots & \ddots & \vdots \\ x_L & x_{L+1} & x_{L+2} & \cdots & x_{\mathrm{N}} \end{pmatrix} \tag{13}$$

3.3.1.2. Decomposition into PCs

At this stage, the covariance matrix of each embedding matrix $\tilde{\mathbf{X}}$ is obtained following Equation (14).

$$\mathbf{C}_X = \frac{\tilde{\mathbf{X}}^t \tilde{\mathbf{X}}}{K} \tag{14}$$

The covariance matrix $\mathbf{C}_X$ is subjected to singular value decomposition according to Equation (15).

$$\boldsymbol{C}_X \boldsymbol{U}_k = \lambda_k \boldsymbol{U}_k \tag{15}$$

L eigenvalues $\boldsymbol{\lambda}_k$ and L corresponding eigenvectors which are ordered as columns of $\mathbf{U}_k$ are obtained in this manner. The eigenvalues $\boldsymbol{\lambda}_k$ are ordered in decreasing order and all eigenvectors in the columns of $\mathbf{U}_k$, are in the same order as their corresponding eigenvalues, so that the first several ones are responsible for a big part of the variance of the data. The PCs are obtained by projecting the embedding matrix onto the eigenvectors:

$$A_k^i(n) = \sum_{l=1}^{L} \tilde{X}^i\,(n + l - 1) U_k(l) \tag{16}$$

Therefore, the eigenvectors corresponding to the baseline/healthy state are arranged as columns of the matrix $\mathbf{U}$ as shown in Equation (17).

$$\boldsymbol{U} = (\boldsymbol{U_1}, \boldsymbol{U_2}, \ldots, \boldsymbol{U_L}) \tag{17}$$

The matrix $\mathbf{U}$ defines the baseline space. This is the full matrix made from all the eigenvectors. Usually, only a few of them are used for further purposes. There are several criteria mentioned in Ref. 16 that can be used for the selection of the number of eigenvectors. However, for the purposes of visualization, in our case the first three eigenvectors are used.

3.3.2. *Fault diagnosis process*

At this stage, new signals are presented and the aim is to diagnose the bearings on which they have been measured. This stage has two main phases: feature extraction and fault identification, which includes fault detection and fault type and size assessment. These are described in the following section:

3.3.2.1. Feature extraction

The fault identification here is done on the basis of certain features. So the first stage is to build these features using the measured signals. This is done by projecting the signal onto the baseline space defined by the matrix $\mathbf{U}$ (see Equations (17) and (18)).

For each new signal i, the embedding matrix $\tilde{\mathbf{X}}^i$ is calculated and then the PCs are obtained by projecting each $\tilde{\mathbf{X}}^i$ onto the $\mathbf{U}_k$ baseline space as shown in Equation (18).

The PCs obtained for each observation signal vector i are arranged into vector-column as shown in Equation (18).

$$\boldsymbol{A}^i = (\boldsymbol{A}_1, \boldsymbol{A}_2, \ldots, \boldsymbol{A}_L) \tag{18}$$

The FVs are calculated by the Euclidean norm of each PC as shown in Equation (19) where $p \leq L$ is the number of PCs considered.

$$T_p^i = \sum_{n=1}^{K} \left(A_p^i(n)\right)^2 \tag{19}$$

Similarly, as in the previous methodology the feature values are arranged into a vector $\mathbf{T}$ with dimension $p \leq L$. The FV $\mathbf{T}$ characterizes the similarity of the observed signal $\mathbf{x}$ to the baseline space, which is based on the healthy bearing scenario.

3.3.2.2. Fault detection

The FVs obtained from the training sample corresponding to the healthy bearing condition are used to make the baseline feature matrix $\mathbf{T}_B$ as defined in Equation (13) (see Section 3.2.4).

The next step is to measure the similarity of an observed feature vector $\mathbf{T}^i = (T_{1,i}, T_{1,i}, T_{p,i})$ to the baseline feature matrix $\mathbf{T}_B$ where i is the number of observation signal vectors considered. This is done on the basis of the Mahalanobis distance of the vector $\mathbf{T}^i$ to the matrix $\mathbf{T}_B$ as defined in Equation (14) (see Section 3.2.4).

Similarly, as in Section 3.2.4., for the purposes of damage detection a threshold ϑ is defined and the obtained Mahalanobis distance D_i is compared with the threshold. If the distance to the baseline matrix is less than $\vartheta, D_i < \vartheta$, then the observed signal vector is assigned to the baseline (healthy) category. If $D_i > \vartheta$, then the newly observed vector is considered to be outside the baseline category, i.e. it belongs to the damaged category.

3.3.2.3. Fault type and size identification

The next two steps of the diagnosis process are the determination of the fault type and its size estimation. They are done in the same way as the detection process. Training samples for each category corresponding to (1) different fault types and to (2) different fault sizes are built using a number of measured signals. Then each new signal, once converted into FV, is compared to these training samples in terms of its Mahalanobis distance. The signal/the FV is assigned to the category to which its Mahalanobis distance is the smallest one. That is, the 1 nearest neighbor (1NN) rule is used to determine the fault type and estimate its size. The fault type diagnosis is done first, and then within each type category, size categories training sets are created. Following the 1NN rule, the fault is assigned to the closest category in terms of its Mahalanobis distance.

3.4. *A case study for structural damage assessment in wind turbine blades*

3.4.1. *The case study*

This section applies the structural damage assessment methodology which was presented in Section 3.2 for a large SSP34 m wind turbine blade. The SSP34 m blade was mounted on a test rig at DTU Wind Energy facilities in Roskilde, Denmark. The data for this study (see Acknowledgement) was provided and belongs to Brüel & Kjær.

In this study, the main objective was to assess the artificially introduced damage in the trailing edge (TE) of the blade. The blade was excited by an electromechanical actuator to invoke a free-decay response. The aim of the analysis was to detect the damage when the blade was excited at different actuation locations. The experiment was performed for the case of sensors placed in different locations along the blade. In this section, the experiment is described and after that certain results that have been obtained are presented using the above described methodology.

Figure 1. The real-scale turbine blade tested.

The SSP34 m blade was mounted in a cantilever position in a test rig as shown in Figure 1. The blade was clamped at the root-end as it would be mounted on the rotor hub of the wind turbine. Twenty B&K tri axial accelerometers Type 4524-B were attached to the blade. 10 of these accelerometers were placed on the leading edge and the other 10 on the TE. The data measured in the direction perpendicular to the blade surface was analyzed. The placement of the accelerometers did not follow any systematic approach for selecting an optimum number and/or location. The excitation was provided by a signal generator, which was set to generate an amplified rectangular pulse fed to the actuator for each actuator hit. The free-decay response of the blade invoked by the applied rectangular pulse force was measured.

To perform the data-driven methodology, a full scale 34-m blade, manufactured by SSP Technology A/S, was mounted to a test rig under laboratory conditions (see Ref. 37 for more information). The debonding of one of the edges (TE or LE) between the top and bottom shell is a common damage which occurs in wind turbine blades. The damage was introduced artificially

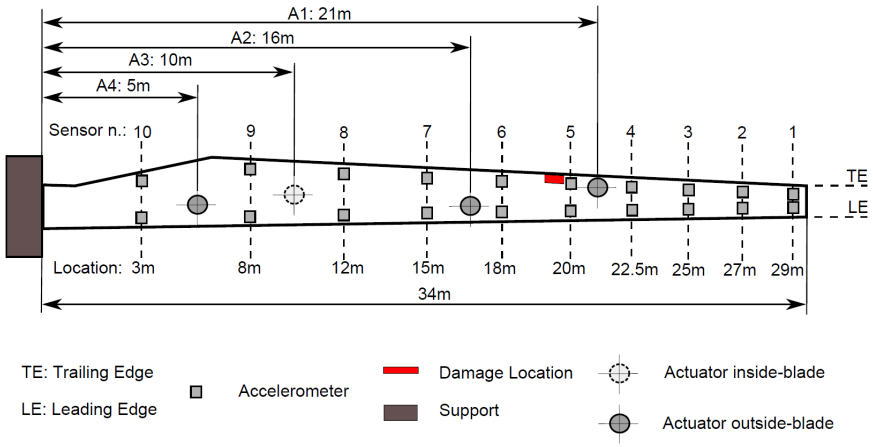

Figure 2. A schematic of the blade with the positions of the damage, the sensors, and the actuators.

into the blade by drilling a series of holes through the glue between the shells of the blade on the TE. Then, using a saw the holes were merged into a crack which was opened by a chisel and a hammer. The crack was gradually extended up to 120 cm.

As mentioned previously, several different actuation positions and several different sensor placements were realized. The damage was also simulated in different locations along the blade. Figure 2 shows the positions of the sensors and actuators and the damage for the scenario tested for which the below results are presented.

3.4.2. *Damage assessment procedure*

The damage detection procedure was separately applied using the data from one sensor at a time. The reason for this is because one of our aims was to analyze the best sensor location for the process.

The reference states were created by the free-decay acceleration response sampled at 16,384 Hz measured for the pristine blade. The reference state was created using $M = 10$ signal vector realizations from the healthy blade and a sliding window size $L = 10$. The vibration responses were transformed into the frequency domain, and discretized into vectors of length $N = 2048$. With these signal vectors, the embedding matrix $\mathbf{Y}$ had a dimension 2048×100. The eigen-decomposition of the covariance matrix of the matrix $\mathbf{Y}$ yielded 100 eigenvalues and their corresponding eigenvectors.

Therefore, the reference space matrix $\mathbf{R}$ (see Section 3.2.2) had a dimension 2048×10.

The FVs were obtained by projecting the observation signal onto the reference space. A dimension of $p = 4$ was utilized for the FVs in this analysis. Thus, only the first four reconstructed components were used to build the baseline FV matrix. The data measured on the healthy blade was divided into two sets, a training set and a testing one, each of which was built using 21 signals/vectors. The training set was used to create the baseline FV matrix where the newly observed FVs are to be compared.

Accordingly, the baseline FV matrix $\mathbf{T}_B$ was constructed by using $s = 21$ FVs with a dimension $p = 4$ (see Section 3.2.2). The Mahalanobis distance of each observation to the baseline matrix $\mathbf{T}_B$ was measured to determine the damage index corresponding to each observation (see Section 3.2.4).

In order to visualize the methodology performance, the damage indices obtained when using the signals from sensor 4 at the TE are presented in Figure 3 when the blade was excited at the different actuator locations. It can be seen that for the four cases, the damaged cases were clearly detected. The number of false alarms (when the blade was not damaged but the system classified it as damaged) and missed damage cases was low for most cases except for a couple of exceptions.

It can be seen from Table 1 that most of the damaged as well as the healthy cases were correctly classified for most actuator and sensor positions. An exception is the healthy cases classified as damaged for the position A3 of the actuator and for a number of the sensor positions. This actuator is inside the blade and is rather far away from the damage. Actuators 1 and 2 are closer to the damage as compared to actuators 3 and 4, and the results for the cases of A1 and A2 are in general better than the results for the actuator positions A3 and A4.

In terms of sensors from Figure 2, it should be appreciated that sensors 5 and 6 are the ones closest to the damage (sensor 5 is the closest one). It can be seen from Table 1 that these sensors give the worst results in terms of identifying the damaged cases, especially for the actuation in position A1, which is also the closest one to the damage.

3.5. *A case study for rolling element fault diagnosis*

This part considers the application of the method for fault assessment described in Section 3.3.

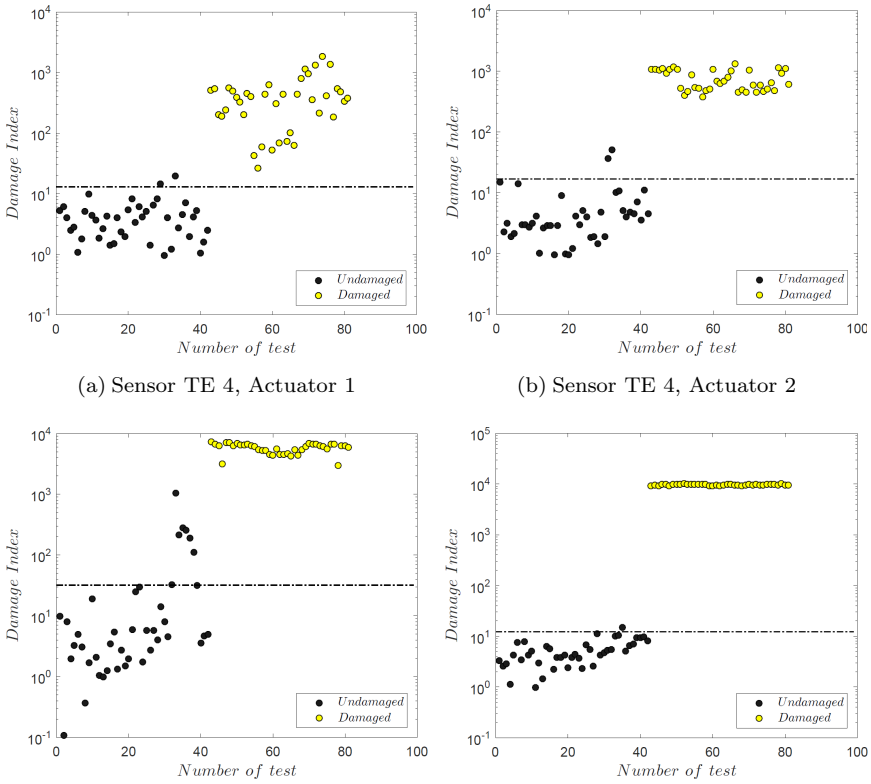

(a) Sensor TE 4, Actuator 1

(b) Sensor TE 4, Actuator 2

(c) Sensor TE 4, Actuator 3

(d) Sensor TE 4, Actuator 4

Figure 3. Mahalanobis distance damage index for different sensors and actuators.

3.5.1. *The case study*

The bearing vibration data were obtained from the test rig of Case Western Reserve University (CWRU). The data-bearing center[38] shown in Figure 4 consists of a 3 HP three-phase induction motor: a dynamometer. The drive end bearing (SKF 6025 deep grove ball bearing) data was used in this analysis. An electrical discharge machine was used to introduce single-point faults in the bearing raceways and ball elements of different bearings with fault diameters of 0.007, 0.014, and 0.021 inches and a depth of 0.011 inches. The bearing vibration data sets were obtained at a sampling rate of 12 kHz for different fault sizes and at speeds varying from 1730 rpm to 1797 rpm. The data for the ORF were taken with

Table 1. Percentage of correct classification of healthy and damaged observations for the SSP34 m-WTB.

		Sensors TE									
Actuator	(%)	1	2	3	4	5	6	7	8	9	10
A1	Correct H	100	98	95	95	100	100	100	100	95	95
	Correct D	100	100	92	100	62	56	100	100	100	100
A2	Correct H	95	86	76	95	98	98	98	86	95	98
	Correct D	100	100	100	100	100	100	100	100	100	100
A3	Correct H	69	74	98	83	83	76	81	83	71	64
	Correct D	100	100	100	100	100	100	100	79	79	72
A4	Correct H	83	100	86	98	79	90	93	88	95	83
	Correct D	100	92	100	100	100	100	100	100	100	69

Notes: In bold and highlighted in grey are the percentages greater than 90% for healthy and damaged observations, respectively. Threshold at risk of false alarm probability equal to $\alpha = 0.01$ for lognormal distribution. The FV dimension is 4 (T1–T4). Total healthy observations = 42, total damaged observations = 39.

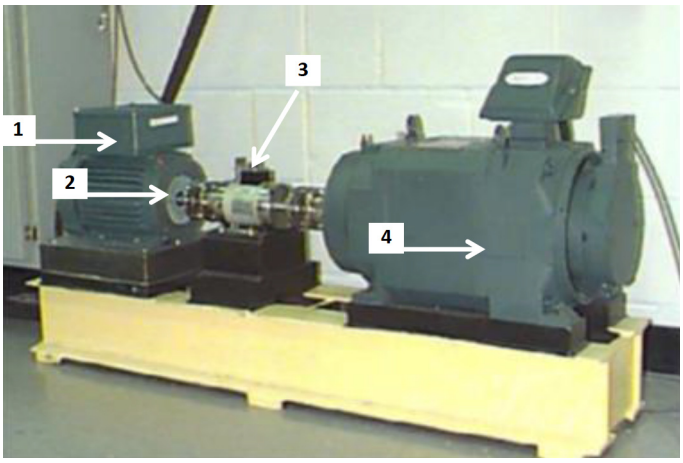

Figure 4. The bearing test rig of CWRU.[38] (1) Induction motor, (2) accelerometer position, (3) torque transducer and (4) dynamometer.

the fault position centered at the 6 o'clock position with respect to the load zone.

The results presented for demonstration are based on the signals obtained at 1730 rpm for a healthy bearing (H), a bearing with an IRF, a bearing with a ball fault (BF) and a bearing with an ORF with a fault size of 0.007 inch in diameter for all the fault types. The first part of the

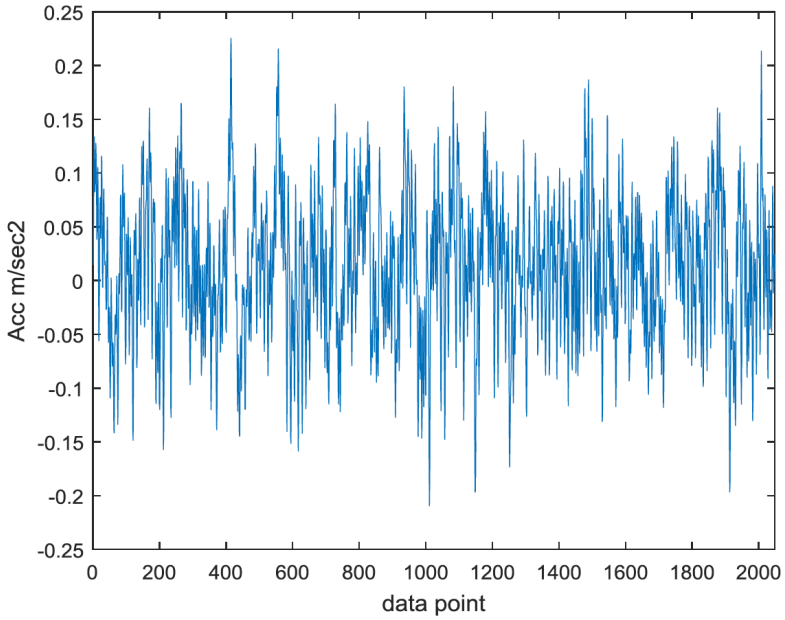

Figure 5. Raw signal from healthy bearing.

diagnosis process is the detection which as explained earlier, is done on the basis of a threshold for the Mahalanobis distance. In this case, the threshold is selected so that 99% of the data from the training sample are below the threshold. Figure 5 presents a raw signal corresponding to a healthy bearing.

3.5.2. *Fault assessment*

3.5.2.1. Fault detection

The decomposition into PCs will result in building the baseline space. For the purposes of visualization only the first three PCs were used, which in this case contained 80% of the total variance of the data, but even with these the results are quite impressive.

Figure 6 presents the baseline data set corresponding to the healthy bearings and the projections of the measured data for the cases of different sizes and different fault types. It can be visually perceived that the classes/sets corresponding to the different fault conditions are very well separated. All the faulty conditions are correctly identified as such — all

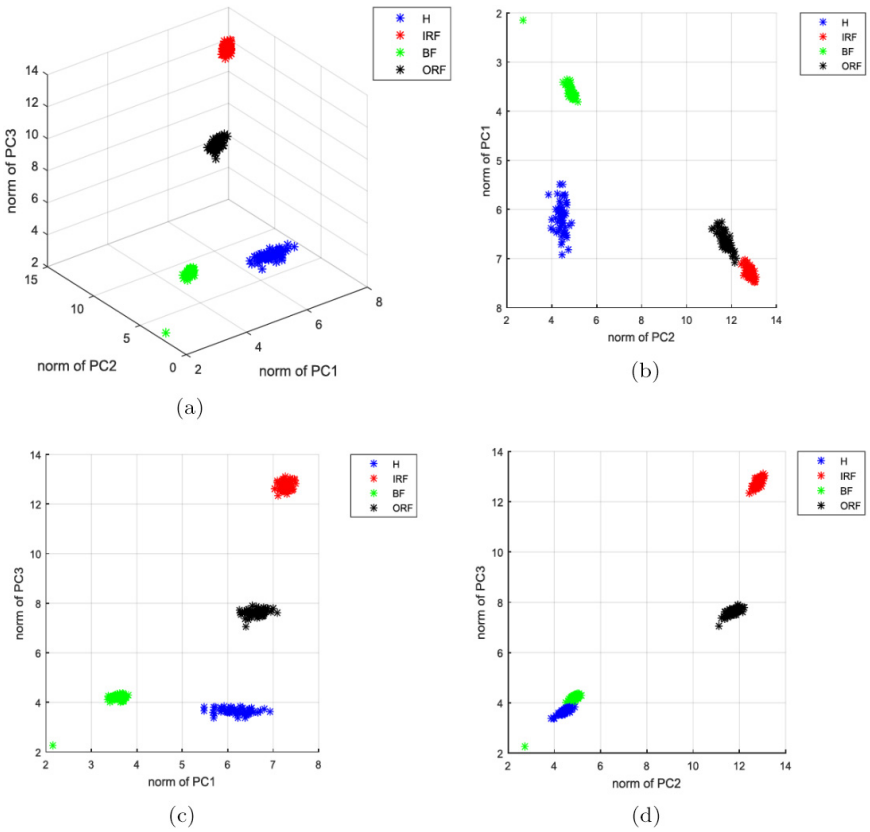

Figure 6. Projection of the signals from different categories on the baseline space.

Table 2. Confusion matrix for the detection of rolling element bearing faults.

Actual/identity class (%)	Healthy	Faulty
Healthy	93.3	6.7
Faulty	0	100

the data corresponding to the three different fault categories — IRF, ORF, and BF are quite away from the set threshold. Table 2 summarizes the detection results. The results are based on the testing sample, which in this case was built using 210 signals, 30 signals from the healthy category and 180 signals from the faulty category. It can be seen that all the faulty cases are correctly identified as faulty. Around 93.3% of the healthy cases

are correctly recognized as healthy, while about 6.7% are miss classified as faulty.

3.5.2.2. Fault identification: Type and size estimation

Once the presence of a fault is established, that is the detection stage is fulfilled, the next two stages are the fault type determination and the fault size estimation. In this particular case, the data one is in possession of are signals from healthy bearings (H), bearings with an IRF, bearings with an ORF, and bearings with a BF. The task at the fault type identification stage is to distinguish between these three categories. As was explained earlier (see Section 3.3.1), this is done using training samples for each of the categories in order to build the corresponding reference spaces/matrices. Then the Mahalanobis distance of a new projection to each of the categories is measured. Eventually, the signal is categorized to the set to which its distance is the smallest one. In this case, half of the measured signal segments corresponding only to small faults (30 signal segments altogether), were used to build a training sample. The rest of the signals, that is $4 \times 30 = 120$ in this case, were used as a testing sample. For rotational speed of 1730 rpm and for the case of three features, i.e. 3 PCs were used to make the baseline space, all the signals from the testing sample were correctly classified. And the confusion matrix is given in Table 3.

It can be appreciated form the results in Table 3 that all the faults from the four different fault type categories were correctly classified to the right category.

Once the type of the fault is established, the fault size was estimated. In this case, the data available was for three different fault sizes — 0.007", 0.014", and 0.021". So these three sizes were assigned to three different categories namely small (S), medium (M), and large faults (L). The size identification is performed the same way as the type identification. That is, training samples were used made of 30 signals from each category. Then,

Table 3. Percentage of correctly classified and missclassified faults for the case of 1730 rpm.

Real/identified fault type (%)	H	IRF	ORF	BF
H	100	0	0	0
IRF	0	100	0	0
ORF	0	0	100	0
BF	0	0	0	100

Table 4. Confusion matrix for size estimation/categorization for IRF 1730 rpm.

Correct/identified fault size (%)	H	S	M	L
H	100	0	0	0
S	0	100	0	0
M	0	0	100	0
L	0	0	0	100

each signal from the testing sample was assigned to its closest category in the sense of Mahalanobis distance. As a demonstration, the confusion matrix for the particular case of rotational speed of 1730 rpm and for the case of IRF is given in Table 4.

It can be seen that all the signals were correctly classified to the right size category.

3.6. *Discussion and conclusions*

This chapter offers a study on the application of data analysis methods for the purposes of vibration-based structural and machinery health and condition monitoring. Data-driven methods which are based on pure data analysis have a lot of potential for monitoring applications in structures and in machinery as they do not assume any model or linearity and thus offer a more general application which can be used for different structures/machinery and for a variety of faults/damages. Therefore, even though the methods considered in this study were developed and tested for particular applications, they can be easily used for different purposes of structural and machinery monitoring.

In particular, the methodology considered is based on SSA, which decomposes the measured vibration signals into new independent components which contain most of the variance of the original data. Eventually, the initial signals can be reconstructed and the precision of the decomposition using different numbers of components can be evaluated. In this study, SSA is applied in different modifications for (1) structural health monitoring and (2) for machinery condition monitoring.

In the first application, a method for detecting structural anomalies (a SHM method) is developed, which uses the reconstructed components and compares them to a reference state/space based on the reconstructed

signals from the healthy/pristine condition of the structure. The method uses a threshold in order to distinguish between signals, measured on the healthy structure and signals measured in a damaged condition.

In the second application, a method for rolling element fault detection and identification is developed, which applies SSA in different ways so that a baseline space is built using the decomposed signals from the healthy/baseline condition. Consequently, a new signal embedded into an embedding matrix is projected onto the baseline space in order to evaluate its similarity to the baseline/healthy condition.

The method for SHM was developed primarily for delamination diagnosis purposes, and the method for machinery diagnosis was specifically developed for rolling element diagnosis purposes. It should be mentioned that the method for structural health monitoring has been applied to a number of applications (although just one is mentioned within this study) including for delamination detection in composite plates[39] and also for a lab-scale turbine blade.[34] It demonstrated very good results for all these applications.

The method for rolling element bearings has been applied for three case studies, two of which are experimental test rigs — one at Strathclyde University and one at the University of Torino.[40] In this study only the application using the data from CWR University is shown as it is most demonstrative in terms of data variety from different fault conditions. But it should be mentioned that the methodology for rolling element fault diagnosis gave very high percentage of correct classification (close to 100%) for all case studies. Thus, it has been validated and verified for different applications of rolling element bearing fault diagnosis. It should be mentioned that this methodology provides a rather simple approach for rolling element bearing fault diagnosis and at least at the first stage, the detection can be quite easily applied if one is in possession of data for the baseline/healthy state only.[35] The subsequent stages for fault type identification and severity estimation as currently developed require data from damaged conditions, which should be usually taken from the same machine. The severity estimation without supervision that is based on the healthy/baseline condition data is under consideration for further research.

The case study for the turbine blade application was primarily developed for the purposes of preliminary research and one of our goals was to test the best position of the application of the excitation and the sensor(s). As can be seen from the results discussed, the method achieves

quite good separation between the faulty and the healthy conditions for most configurations of the sensors and the actuators. The separation is not good when both/or any — the sensor and/or the actuator — are close to the damage. The best results are obtained when both the sensor and the actuator are not very close but they are also not too far away from the damage. Out best results are for sensors 2, 3, and 4 when the damage is between sensors 5 and 6 and for actuation point 3. More research is needed in order to develop the method to an application stage.

Future research in the directions of application of SSA for the purposes of machinery and structural health monitoring will be oriented in two main areas: the development of better classification and diagnosis methods and the development of fully applied methods that can be incorporated for practical monitoring. The methods used for classification purposes as presented earlier in this chapter can be further developed in order to make the process easier and more automatic. Pattern recognition methods can be applied and e.g. linear or nonlinear boundaries between the different classes can be designed for the purposes of recognition. Also, the development of more unsupervised methods when there is no or minimal information about the damaged states for the machinery and the structural diagnosis are needed.

Acknowledgement

The authors acknowledge the help and the collaboration with Dr Dmitri Tcherniak from Brüel & Kjær S/V Measurements who did the experiment with the turbine blade and kindly provided the data.

References

1. Doebling, S. W., Farrar, C. R., Prime, M. B., and Shevitz, D. W. Damage identification and health monitoring of structural and mechanical systems from changes in their vibration characteristics: A literature review; Los Alamos National Lab., NM (United States) (1996).
2. Carden, E. P., and Fanning, P. Vibration based condition monitoring: A review. *Structural Health Monitoring* **3**(4), 355–377 (2004).
3. Worden, K., and Manson, G. The application of machine learning to structural health monitoring. *Philosophical Transactions of the Royal Society of London A: Mathematical, Physical and Engineering Sciences* **365**(1851), 515–537 (2007).
4. Sohn, H., and Farrar, C. R. Damage diagnosis using time series analysis of vibration signals. *Smart Materials and Structures* **10**(3), 446 (2001).
5. Bishop, C. M. *Neural Networks for Pattern Recognition*. Oxford University Press (1995).

6. Yao, R., and Pakzad, S. N. Autoregressive statistical pattern recognition algorithms for damage detection in civil structures. *Mechanical Systems and Signal Processing* **31**, 355–368 (2012).
7. Tandon, N., and Choudhury, A. A review of vibration and acoustic measurement methods for the detection of defects in rolling element bearings. *Tribology International* **32**(8), 469–480 (1999).
8. Basseville, M., Mevel, L., and Goursat, M. Statistical model-based damage detection and localization: subspace-based residuals and damage-to-noise sensitivity ratios. *Journal of Sound and Vibration* **275**(3), 769–794 (2004).
9. Kopsaftopoulos, F., and Fassois, S. Vibration based health monitoring for a lightweight truss structure: Experimental assessment of several statistical time series methods. *Mechanical Systems and Signal Processing* **24**(7), 1977–1997 (2010).
10. Taylor, S. J. Modelling Financial Time Series, 2007.
11. Wei, W. W.-S. *Time Series Analysis*. Addison-Wesley, Reading (1994).
12. Hassani, H. Singular Spectrum Analysis: Methodology and Comparison. (2007).
13. Jolliffe, I. *Principal Component Analysis*. Wiley, Online Library (2002).
14. Mujica, L., Rodellar, J., Fernandez, A., and Guemes, A. Q-statistic and T2-statistic PCA-based measures for damage assessment in structures. *Structural Health Monitoring* 1475921710388972 (2010).
15. Johnson, M. Waveform based clustering and classification of AE transients in composite laminates using principal component analysis. *NDT & E International* **35**(3), 367–376 (2002).
16. Kilundu, B., Chiementin, X., and Dehombreux, P. Singular spectrum analysis for bearing defect detection. *Journal of Vibration and Acoustics* **133**(5), 051007 (2011).
17. Muruganatham, B., Sanjith, M., Krishnakumar, B., and Satya Murty, S. Roller element bearing fault diagnosis using singular spectrum analysis. *Mechanical Systems and Signal Processing* **35**(1), 150–166 (2013).
18. Lopez, I., and Sarigul-Klijn, N. Effects of dimensional reduction techniques on structural damage assessment under uncertainty. *Journal of Vibration and Acoustics* **133**(6), 061008 (2011).
19. Yan, A.-M., Kerschen, G., De Boe, P., and Golinval, J.-C. Structural damage diagnosis under varying environmental conditions — part I: A linear analysis. *Mechanical Systems and Signal Processing* **19**(4), 847–864 (2005).
20. Yan, A.-M., Kerschen, G., De Boe, P., and Golinval, J.-C. Structural damage diagnosis under varying environmental conditions — part II: Local PCA for non-linear cases. *Mechanical Systems and Signal Processing* **19**(4), 865–880 (2005).
21. González, A. G., and Fassois, S. A supervised vibration-based statistical methodology for damage detection under varying environmental conditions & its laboratory assessment with a scale wind turbine blade. *Journal of Sound and Vibration* **366**, 484–500 (2016).
22. Ghil, M., Allen, M., Dettinger, M., Ide, K., Kondrashov, D., Mann, M., Robertson, A. W., Saunders, A., Tian, Y., and Varadi, F. Advanced spectral

methods for climatic time series. *Reviews of Geophysics* **40**(1), 3-1–3-41 (2002).
23. Basilevsky, A., and Hum, D. P. Karhunen-Loeve analysis of historical time series with an application to plantation births in Jamaica. *Journal of the American Statistical Association* **74**(366a), 284–290 (1979).
24. Hassani, H., and Thomakos, D. A review on singular spectrum analysis for economic and financial time series. *Statistics and its Interface* **3**(3), 377–397 (2010).
25. Yiou, P., Sornette, D., and Ghil, M. Data-adaptive wavelets and multi-scale singular-spectrum analysis. *Physica D: Nonlinear Phenomena* **142**(3), 254–290 (2000).
26. Loh, C.-H., Tseng, M.-H., and Chao, S.-H. Structural Damage Assessment Using Output-Only Measurement: Localization and Quantification. In *ASME 2013 Conference on Smart Materials, Adaptive Structures and Intelligent Systems*, American Society of Mechanical Engineers, pp. V002T05A001–V002T05A001 (2013).
27. Chao, S.-H., and Loh, C.-H. Application of singular spectrum analysis to structural monitoring and damage diagnosis of bridges. *Structure and Infrastructure Engineering* **10**(6), 708–727 (2014).
28. Salgado, D., and Alonso, F. Tool wear detection in turning operations using singular spectrum analysis. *Journal of Materials Processing Technology* **171**(3), 451–458 (2006).
29. Kilundu, B., Dehombreux, P., and Chiementin, X. Tool wear monitoring by machine learning techniques and singular spectrum analysis. *Mechanical Systems and Signal Processing* **25**(1), 400–415 (2011).
30. Muruganatham, B., Sanjith, M., Kumar, B. K., Murty, S., and Swaminathan, P. Inner Race Bearing Fault Detection Using Singular Spectrum Analysis. In *Communication Control and Computing Technologies* (*ICCCCT*), International Conference on 2010 IEEE, pp. 573–579 (2010).
31. Garcia, D., and Trendafilova, I. A multivariate data analysis approach towards vibration analysis and vibration-based damage assessment: Application for delamination detection in a composite beam. *Journal of Sound and Vibration* **333**(25), 7036–7050 (2014).
32. Zabalza, J., Ren, J., Zheng, J., Han, J., Zhao, H., Li, S., and Marshall, S. Novel two-dimensional singular spectrum analysis for effective feature extraction and data classification in hyperspectral imaging. *IEEE Transactions on Geoscience and Remote Sensing* **53**(8), 4418–4433 (2015).
33. Sohn, H., Czarnecki, J. A., and Farrar, C. R. Structural health monitoring using statistical process control. *Journal of Structural Engineering* **126**(11), 1356–1363 (2000).
34. García, D., Tcherniak, D., and Trendafilova, I. Damage assessment for wind turbine blades based on a multivariate statistical approach, *Journal of Physics: Conference Series*, p. 012086 (2015).
35. Al-Bugharbee, H. R. S. Data-driven methodologies for bearing vibration analysis and vibration based fault diagnosis. University of Strathclyde (2016).

36. Kantz, H., and Schreiber, T. *Nonlinear Time Series Analysis*. Cambridge University Press, Vol. 7 (2004).
37. Larsen, G. C., Berring, P., Tcherniak, D., Nielsen, P. H., and Branner, K. Effect of a Damage to Modal Parameters of a Wind Turbine Blade. In *EWSHM-7th European Workshop on Structural Health Monitoring* (2014).
38. CWRUBDCW, The Case Western Reserve University Bearing Data Center Website (2014).
39. Palazzetti, R., Garcia, D., Trendafilova, I., Fiorini, C., and Zucchelli, A. An Investigation in Vibration Modelling and Vibration-based Monitoring for Composite Laminates. In *26th International Conference on Noise and Vibration Engineering* (2014).
40. Tabrizi, A. A., Al-Bugharbee, H., Trendafilova, I., and Garibaldi, L. A cointegration-based monitoring method for rolling bearings working in time-varying operational conditions. *Meccanica*, 1–17.